University of California

Ernest O. Lawrence Radiation Laboratory

TWO-WEEK LOAN COPY

This is a Library Circulating Copy which may be borrowed for two weeks. For a personal retention copy, call Tech. Info. Division, Ext. 5545

Berkeley, California

DISCLAIMER

This document was prepared as an account of work sponsored by the United States Government. While this document is believed to contain correct information, neither the United States Government nor any agency thereof, nor the Regents of the University of California, nor any of their employees, makes any warranty, express or implied, or assumes any legal responsibility for the accuracy, completeness, or usefulness of any information, apparatus, product, or process disclosed, or represents that its use would not infringe privately owned rights. Reference herein to any specific commercial product, process, or service by its trade name, trademark, manufacturer, or otherwise, does not necessarily constitute or imply its endorsement, recommendation, or favoring by the United States Government or any agency thereof, or the Regents of the University of California. The views and opinions of authors expressed herein do not necessarily state or reflect those of the United States Government or any agency thereof or the Regents of the University of California.

Proceedings of Am. Inst. of Chem. Engineers
Meeting

UCRL-9787
Revised

UNIVERSITY OF CALIFORNIA

Lawrence Radiation Laboratory
Berkeley, California

Contract No. W-7405-eng-48

BULK MIXING OF IMMISCIBLE LIQUIDS IN BAFFLED CYLINDRICAL TANKS

L. H. Weiss, J. L. Fick, R. H. Houston, and T. Vermeulen

October 8, 1962

UCRL-9787
- Revised.

BULK MIXING OF IMMISCIBLE LIQUIDS IN BAFFLED CYLINDRICAL TANKS

L. H. Weiss, J. L. Fick, R. H. Houston, and T. Vermeulen
University of California, Berkeley 4, California

ABSTRACT

Two factors account for incomplete bulk mixing of immiscible liquids: partial settling of droplets in the emulsion phase, and resistance to breakup by residual second phase. In the present experimentally-based quantitative treatment, the first effect depends upon Froude, Reynolds, and Weber numbers; the second, upon Weber number alone.

* * * *

For presentation at a meeting of the American Institute of Chemical Engineers. Not to be published without permission of A.I.Ch.E. and the authors.

Because mixing of immiscible liquids is usually undertaken to bring about a transfer of material between the phases, three primary objectives of the process can be identified: homogeneous bulk mixing, which ensures adequate contacting of the inter-suspended phases; turbulence around and within the droplets, which directly reduces resistance to mass transfer; and a large interfacial area, which also promotes interphase transport. In terms of the fluid mechanics of the process, these three goals are closely related. Nevertheless, attainment of any one of them does not necessarily indicate satisfactory levels for the other two.

Bulk inhomogeneity, between samples large compared to droplet volume but small relative to tank volume, is the concern of this article. Two types of inhomogeneity occur which are directly related to each other:

1. Vertical segregation within the emulsified continuous phase.

2. Undispersed second phase present as a discrete layer.

The first type is a result of insufficient circulation and turbulence. The second type results from agitation too weak to complete the dispersion process. The conventional mixing index (3,6) or modifications of it (2) do not distinguish adequately between these two effects.

If radial variation in bulk composition is small compared to the vertical variation, the dispersion can be described as a property solely of height in the containing vessel. Figure 1 shows the range of possible distributions of the local volume

fraction φ_s, as a function of fractional tank height h, with h = 0 at the end of the tank where the settled dispersible phase would lie. Curve A represents no mixing whatever, and has somewhat the appearance of a cross-section view of a stagnant agitator. Curve B represents the opposite extreme, complete bulk homogeneity, with a sample anywhere in the vessel identical to the overall composition $\bar{\varphi}$. The other curves in Figure 1 represent one type of intermediate distributions.

It is evident from physical considerations that an upper limit exists for the concentration, φ_s, of dispersed phase in the emulsion; this limiting value is taken here to be 0.70. With poor mixing, both a stagnant layer of second phase and a steep gradient for φ_s within the emulsion are likely to occur. The highest value of φ_s (i.e., φ_{max}) will occur at an interface with the undispersed material, if any, at $h = h_B$. The value of h_B represents the relative volume of second phase that is not participating at all in the mixing process; for "good" mixing, $h_B = 0$.

An exponential relation for the gradient in the emulsion is suggested by the Boltzmann distribution of molecules in a gravitational field:

$$\frac{\varphi_s}{\varphi_{max}} = e^{-\kappa(h - h_B)} \tag{1}$$

where κ is an "inhomogeneity parameter". In order to satisfy a material balance, we have

$$\bar{\varphi} = h_B + \varphi_{max} \int_{h_B}^{1.0} e^{-\kappa(h - h_B)} dh \tag{2}$$

The parameters of Equation 1 are illustrated in Figure 2. An extrapolated volume fraction φ_{lim}, also shown, is useful in

calculating κ and h_B from experimental profiles of φ_s.

The slope κ varies from zero at perfect mixing, to infinity at no mixing. A "theoretical mixing index", TMI, can then be defined as:

$$\text{TMI} = \frac{1}{1 + \kappa} \tag{3}$$

The function 100 (TMI) thus indicates a percentage of approach to complete mixing in the emulsion layer.

The two parameters h_B and κ, defined by their use in Equations 1 and 2, can be examined independently, in order to provide a more accurate definition of bulk mixing than was previously available.

DEVELOPMENT OF THE TWO-PARAMETER MODEL

Theory for κ

If the analogy with the Boltzmann statistical model is pursued, κ can be considered to depend upon the square of the ratio V_p/V_j of relative local particle velocity to the velocity of the surrounding continuous phase. For an agitated mixture in a square cylindrical tank, the turbine impeller acts to form a jet of fluid with a velocity nearly equal to the tip speed, πNL. This jet in turn causes circulation throughout the tank. The average local velocity at any other point should be related to the tip speed by the ratio of initial jet area, LW (impeller diameter times impeller width) to tank cross-sectional area TH (diameter times height) to allow for the decrease in velocity with distance from the impeller. Therefore, the average local velocity should be proportional to impeller-tip speed and to a power (a) of the geometrical group, G = LW/TH:

$$V_j \propto (NL)\ G^a \tag{4}$$

It is postulated now that the mean velocity of particles relative to the continuous phase will be proportional to the terminal settling velocity of the system. In the general case, this is

$$V_p = \text{const.}\left(\frac{g|\Delta\rho|(1-\bar{\varphi})d_p}{\bar{\rho}}\right)^{1-n}\left(\frac{d_p\,\bar{\rho}}{\mu_m}\right)^{1-2n} \tag{5}$$

where $\bar{\rho}$ is mixture density, $\Delta\rho$ is density difference between the dispersible and continuous phases, g is gravitational acceleration, μ is mixture viscosity (see Notation), and d_p is mean droplet diameter. For laminar flow, n = 0; and for isotropic turbulence, n = 0.5. Combination of Equations (4) and (5) yields:

$$\kappa^{-1} \propto (N_{Fr})^{2-2n}\ (N_{Re})^{-2+4n}\left(\frac{L}{d_p}\right)^{4-6n} G^{2a} \tag{6}$$

where $N_{Fr} = N^2L\bar{\rho}/g|\Delta\rho|\,(1-\varphi)$; and $N_{Re} = NL^2\bar{\rho}/\mu_m$.

If n is greater than 0.5, the effect of Reynolds number is for an increase in continuous-phase viscosity to hinder the attainment of homogeneity. Below 0.5 the opposite effect will apply. (It will be seen later that n = 0.57.)

Mean droplet diameter d_p has been investigated by Langlois and co-workers (5,15), Rea et al. (12), Fick et al. (2), and Vanderveen (14), resulting in a correlation that depends upon the bulk average volume-fraction $\bar{\varphi}$ of dispersed phase, and the Weber number, $N_{We} = N^2L^3\rho/\sigma$, where σ is the interfacial tension. These results give d_o, the mean droplet diameter at the impeller tip, to be

$$d_o = 0.055\ L\ N_{We}^{-0.60}\ (1 + 2.5\bar{\varphi}) \tag{7}$$

with d_p at any other point equal to d_o plus a correction term for coalescence (14).

Theory for h_B

The stagnant layer represented by h_B can occur as a result of two distinct types of behavior:

First, inability of the emulsified phase to contain more dispersed phase. In this case, φ_{max} will reach a limiting value of around 0.70, and the entire bulk-mixing behavior can be described by the value of κ. This condition will be identified as kappa-controlled.

Second, inability of the main fluid motion to bring about dispersion of the residual liquid. With the impeller entirely within the continuous phase, as agitation commences and a portion of the second phase is dispersed, the interface evidently migrates toward the end of the vessel. At the slower impeller-tip velocities, a point will be reached at which the relative velocity at the interface is insufficient to promote further dispersion. This condition is considered to be dispersion-controlled.

Dispersion has been postulated to occur in three steps (1):

1. An initial disturbance at the interface in the form of a wave.

2. The formation of ligaments which break off from the wave crests.

3. The continued breakup of these fragments into small droplets.

Many previous investigations have shown that dispersion phenomena can be described in terms of the Reynolds, Weber, and Froude groups identified above. Here as before, the inertial force is related to impeller-tip velocity by the geometrical group G. The physical properties of the emulsified portion are influenced

by its composition and hence by $\bar{\varphi}$. Taken together, these considerations indicate that a likely functional form for h_B, when dispersion-controlled, is

$$h_B = \text{fn.}\ (N_{Re},\ N_{We},\ N_{Fr},\ G,\ \bar{\varphi}) \tag{8}$$

Behavior of the Parameters

A criterion can now be developed to determine where the occurrence of non-zero h_B will be kappa-controlled. Integration of the material balance (Equation 2) yields:

$$\bar{\varphi} = h_B + \frac{\varphi_{max}}{\kappa}\left[1 - e^{-\kappa\,(1\,-\,h_B)}\right] \tag{9}$$

Setting $h_B = 0$, and $\varphi_{max} = 0.70$, leads to

$$\bar{\varphi} = \frac{0.70}{\kappa}\left[1 - e^{-\kappa}\right] \tag{10}$$

Equation 10 can be solved iteratively to give the lower-limit values for κ that will give kappa-control of the presence of an undispersed layer. The solution for a range of values for $\bar{\varphi}$ was carried out on the IBM 650 computer, with the results shown in Figure 3.

In practice it will be exceedingly difficult to obtain mixing conditions where $\bar{\varphi}$ exceeds 0.60. To obtain any value of $\bar{\varphi}$ above 0.50, care must be taken to locate the impeller within the phase that is intended to be continuous. Even then, phase inversion may occur in a continuous-flow system.

As a more specific indication of the effect of kappa-controlled coalescence, distribution curves of φ_s are shown in Figure 4 for various values of κ, with $\bar{\varphi} = 0.50$. As κ increases above the limiting value, more and more of the second phase coalesces; the curves cross each other as a consequence of the material balance. The differences between the limitations of incomplete dispersion

and varying uniformity may be seen by comparing Figure 1 with Figure 4.

The consequences of dispersion-controlled mixing have also been explored in some detail. For this purpose, Equation 9 was rewritten in the form:

$$\varphi_{max} = \frac{(\bar{\varphi} - h_B)\,\kappa}{\left[1 - e^{-\kappa(1 - h_B)}\right]}, \text{ with } \varphi_{max} < 0.70 \qquad (11)$$

Values of φ_{max} were then computed for a range of values of κ and h_B, for representative values of $\bar{\varphi}$ (0.1, 0.3, and 0.5) which are shown in Figures 5a, b, and c respectively. This set of graphs is useful for interpolation and short-range extrapolation to other $\bar{\varphi}$ values. For constant values of h_B and $\bar{\varphi}$, φ_{max} increases to its limit of 0.70 with increasing values for κ. For constant values of h_B and κ, φ_{max} increases with $\bar{\varphi}$. For any constant values of $\bar{\varphi}$ and κ, φ_{max} increases as h_B decreases. As κ decreases toward zero, φ_{max} approaches the asymptotic value, $\bar{\varphi} - h_B$.

EXPERIMENTAL PROGRAM

The mixing vessels used in these studies were a cylindrical stainless-steel tank 20 inches in height and diameter, and a smaller stainless-steel tank (nominal 10-inch), also cylindrical, 8.87 inches in height and 10.35 inches in diameter; the vessels were mounted on the same stand, shown in Figure 6. Each tank was equipped with four vertical baffles, each one-tenth the tank diameter in width, at 90° intervals around the tank wall and perpendicular to it. The impellers were four-bladed flat paddles of stainless steel, centered axially and vertically in the tanks.

For each tank a cork gasket between bolted flanges sealed the vessel to its cover, and a mercury seal on the impeller shaft rendered the assembled unit liquid-and-air-tight. A coil of 1/4 inch o.d. copper tubing was soldered to the outside to allow circulation of cooling water for temperature control to 20.0 ± 0.5°C. The impellers for both tanks were driven by a V-belt drive connected to a 3/4-hp. Electra gear motor. Step-cone pulleys on the impeller shafts and the motor shaft enabled the impellers to rotate at fixed speeds of 1.83, 2.83, 4.50 and 6.83 rps.

The sampling probe used was a length of stainless-steel tubing 3/16-inch o.d. and 1/32-inch i.d., ending in a horizontal arm 5.5 inches long. Initially, an array of sampling points was adopted comprising five radial positions at each of six tank heights. Typical measurements along a radius of the tank at several fractional tank heights are shown in Figure 7. After it became apparent that radial fluctuations in concentration were negligible compared with the stratification effects, the sampling array was revised to include ten different heights but only two radial locations. Further data on the experimental conditions are given in a Lawrence Radiation Laboratory report (17).

At each mean volume fraction, two complete profiles were made for each impeller speed; one set was made while increasing the speed and another while decreasing it, after fifteen minutes of equilibration time at any one speed in each case. In the sampling procedure, 10 to 12 cm^3 were withdrawn, transferred to a calibrated centrifuge cone, and centrifuged at 1200 rpm. The volumes of the separated phases were then recorded. Subse-

quently the sample was returned to the tank, in order to avoid depletion and altering of the mean volume-fraction.

The liquids investigated are listed in Table I, and the geometrical variables used appear in Table II.

RESULTS

The concept of dynamic equilibrium for the mixing operation, which involves steady levels of concentration at various points, was confirmed by the results for numerous pairs of duplicate runs. In the vertical direction, the observed distribution of φ_s values corresponded to the type predicted by Equation (1) and illustrated in Figures 1 and 2. After the exponential relation of Equation 1 had been adopted, a least-squares fit to the data for each run was computed on the IBM 650. Dimensionless groups to be used in subsequent correlations were also calculated.

The dimensionless groups in Equation 6 were used in a linear-regression analysis for κ, also carried out on the IBM 650 computer. The optimum result, with a correlation coefficient of 0.83 for 42 runs, was:

$$\ln \kappa = 3.39 \pm 1.09 - (0.232 \pm 0.040) \ln \left[N_{Fr}^{3} \left(\frac{L}{d_p}\right)^2 N_{Re} G^{3/2} \right] \qquad (12)$$

Since the theoretical form for κ was based upon $(V_s/V_j)^2$, the coefficient of the independent variable in Equation 12 should be 2/7, which lies slightly above the prediction interval. A relation of this type is shown in Figure 8, as a solid line fitting the equation:

$$\kappa = 88 \left[(N_{Fr})^3 (N_{Re}) (L/d_p)^2 G^{3/2} \right]^{-2/7} \qquad (13)$$

Equation 13 is seen to correspond exactly to Equation 6, for the case where n = 4/7. In order to eliminate d_p, we can apply Equation 7, with a numerical factor of 2.0 to account for the average

Table I

Physical Properties of Liquids Studied*

Liquid	Density (gm/cm^3)	Viscosity (cp)	Interfacial Tension** (dynes/cm)
Water	0.998	1.00	----
Kerosene	0.803	2.69	43.6
Carbon Tetrachloride	1.60	0.99	38.0
Methyl Isobutyl Ketone	0.800	0.585	12.0
White Oil	0.875	75.0	48.0

*All measurements made at 20°C.

**Interfacial tension determined with water as the second phase.

Table II

Impeller and Tank Dimensions Used

Impeller Length (inches)	Impeller Width (inches)	Tank Diameter (inches)	Tank Height (inches)
2.50	0.94	10.35	8.87
5.00	0.94	"	"
7.50	0.94	"	"
6.77	1.65	"	"
5.00	2.00	20.0	20.0
6.67	2.00	"	"
10.00	2.00	"	"

extent of coalescence. Thus,

$$\kappa = 25 \left[(N_{Fr})^3 (N_{Re}) (N_{We})^{1.2} G^{3/2} (1 + 2.5\varphi)^{-2}\right]^{-2/7} \quad (13a)$$

The dashed line in Figure 8 represents a slightly rounded form of the optimum statistical result:

$$\kappa = 48 \left[(N_{Fr})^3 (N_{Re}) (L/d_p)^2 G^{3/2}\right]^{-1/4} \quad (14)$$

Of these two relations, Equation 13 is somewhat preferred, because of its somewhat firmer theoretical basis. A few data points from the preliminary studies, observed at the highest mixing speed, were dropped from Figure 8 because of strong evidence that centrifugation occurred which was not considered in the models developed here.

Values of $h_B/\bar{\varphi}$ were correlated with the parameters of Equation 8, again using linear regression. The dependent variable was chosen as $h_B/\bar{\varphi}$, rather than h_B, to normalize its range of values between 0 and 1.

The regression runs showed h_B to be almost completely insensitive to N_{Re}. Moreover, N_{Fr} used only with G gave a poorer fit (0.71 correlation coefficient) than N_{We} with G, which showed a correlation coefficient of 0.79. The result for 28 runs, excluding those where $h_B/\varphi = 0$, was:

$$\frac{h_B}{\bar{\varphi}} = 1.683 \pm 0.663 - (0.271 \pm 0.066) \ln N_{We} - (0.194 \pm 0.132) \ln G \quad (15)$$

A separate regression restricted to 12 runs from the detailed studies showed a larger coefficient for $\ln N_{We}$ (-0.365 ± 0.103), and a correlation coefficient of 0.94. This result, weighed with the zero-value $h_B/\bar{\varphi}$ points, indicated that a still steeper slope on N_{We} would be justified. As shown in Figure 9, the preferred correlation is:

$$\frac{h_B}{\overline{\varphi}} = 2.31 - 0.61 \ln (N_{We} G^{0.7}) \tag{16}$$

Since it is not known whether a correlation for $h_B/\overline{\varphi}$ is theoretically more appropriate than for h_B alone, a relation for the latter was derived directly from Equation 16, using $\overline{\varphi} = 0.2$ as a mean value:

$$h_B = 0.66 - 0.12 \ln (N_{We} G^{0.7}/\overline{\varphi}) \tag{17}$$

Strictly, the foregoing equations are applicable only to four-bladed flat paddles, in fully-baffled enclosed cylindrical tanks whose height and diameter are about equal. However, for such vessels, it seems likely that these equations can apply to other impellers having a given diameter and width, by scaling the speed in proportion to the cube root of the power input (13). Hence, for a vaned-disk impeller with four blades, the equations should apply directly; for one with six blades, the effective N to use in the correlations is about 1.11 times the actual value.

DISCUSSION

Conditions Giving Kappa-Control

In designing an agitator, it is generally essential to choose parameters for Equation 15 which will give $h_B = 0$. It is also necessary to choose κ smaller than the limiting value that will give $\varphi_{max} = 0.70$.

If $\sigma^{3.5}/|\Delta\rho|^3 \mu_m$ is less than a constant term (17) for any one system, which can be derived from Equations 13 and 15, the behavior of the system in the practical range of speeds can be calculated entirely from kappa-control considerations. If $\sigma^{3.5}/|\Delta\rho|^3\mu_m$ is greater than the constant term, Figure 10 (also derived from Equation 13 and 15) can be used. This figure shows the ratio of the agitator speed at any given $h_B/\overline{\varphi}$ to the speed that would give

$h_B = 0$, for both dispersion-control and kappa-control.

Each curve is plotted on its own relative-speed scale. Replotting them on an absolute-speed scale would always have the kappa-controlled curves displaced to either the right or the left of the dispersion-controlled curve. Whichever curve lies above the other will control the mixing behavior.

Thus, at the lowest speeds, dispersion will always control. If the dispersion-controlled curve intersects the kappa-controlled curve, the system will shift to the latter as the speed increases. Then, because of the convex shape of the kappa-controlled curves, it is possible to shift back to dispersion control before h_B reaches zero. The larger the group $\sigma^{3.5}/|\Delta\rho|^3\mu_m$ becomes, the larger the relative shift of the kappa-controlled curve to the left in Figure 13, and the greater the likelihood that h_B will be determined entirely by dispersion-control.

Comparison with other results

For solid-liquid systems, Nagata et al. (7,8) and Kneule (4) have established that mass-transfer rates are optimal relative to power input when all the solid particles have just been suspended, thus obviating the need to attain complete bulk homogeneity.

This work led Zwietering (18) to investigate the conditions which will just suspend all the particles in fully baffled vessels. Nagata (7) conducted a similar study in unbaffled tanks.

The critical speed at which solid-liquid systems reach essentially constant composition in baffled vessels was determined by Oyama and Endoh (9). In their runs, solids loading was limited to 1% by weight or lower. Pavlushenko and co-workers (10)

investigated the same standard of homogeneity, but in an unbaffled tank with solids loadings from 20 to 50% by weight.

Weisman and Efferding (16) considered the ratio of slurry-bed height to total liquid height in a baffled vessel. Their condition of incomplete slurry expansion is analogous to the distribution shown in Figure 4, above, for $\kappa = 10$.

An extensive study of conditions for uniformity in seven different immiscible-liquid systems has been carried out by Pavlushenko and Yanishevskii (11), under both baffled and unbaffled conditions; light-transmission measurements were used to determine the approach to homogeneity.

The results of the foregoing studies have been recast into the general form of Equation 6, to provide direct comparisons with the present study. The respective exponents are shown in Table III. The variations in exponents are probably due to differences in both the type of measurements and their respective accuracy. However, several of the criteria adopted appear to be related closely to the parameter κ.

Design of Equipment

The capacity of an agitator can readily be determined from production requirements. However, the optimum choice of an impeller is governed by the following criteria:

(a) For power consumption (12),

$$N^3 L^4 W = \text{a minimum}$$

(b) For drop diameter, determined by turbulent breakup (15),

$$N^{1.2} L^{0.8} \gtrsim \text{a constant}$$

(c) For drop diameter, determined by coalescence (14),

$$N^{0.65} L^{-0.15} \gtrsim \text{a constant}$$

Table III

Comparison of Homogeneity Criteria

Investigator	Dispersed Phase	n value from N_{Re} or N_{Fr}	n value from L/d_p
	Baffled Tanks		
Zwietering (18)	Solid	0.55	0.60
Oyama-Endoh (9)	Solid	0.50	0.61
Weisman-Efferding (16)	Solid	0.33	0.44
Pavlushenko et al. (11)	Liquid	0.81	0.61*
Present Study	Liquid	0.57	0.57
	Unbaffled Tanks		
Pavlushenko et al. (10)	Solid	0.40	0.53
Nagata et al. (8)	Solid	0.44	0.56

*N_{We} effect is recomputed by assuming $L/d_p \propto N_{We}^{0.60}$ (neglecting coalescence effects).

(d) For uniformity within the dispersion (from this study),

$$N^{2.7}L^{2.9}W^{0.43} \geq \text{a constant}$$

(e) For elimination of the unmixed phase,

$$N^{2}L^{3.7}W^{0.7} \geq \text{a constant}$$

Some two of conditions (b) through (e) will be found to control the design: in those conditions the equality will apply, while the remaining two will be overdesigned. For illustrative purposes, let conditions (d) and (e) be considered. The first objective is to determine the optimum values of L and W; combination of (d) and (e) gives:

$$N^{3}L^{1.7}W^{0.10} = \text{a constant}$$

Combination of this with (a) results in:

$$L^{2.6}W = \text{a minimum}$$

With regard to condition (d), $\kappa = 0.10$ should ensure deviations of less than 5% between φ_s and $\bar{\varphi}$, and thus ensure dispersion-control of h_B. At κ less than 0.10, centrifugation effects become important.

Acknowledgment

Thanks are due Homer E. Rea, Jr., and Fred L. Toby for the design of the agitation apparatus used, and to Gardiner G. Young for work connected with its construction. Eugene J. Fenech and Robert S. Brown provided the linear-regression computation program. The entire investigation was performed under the auspices of the U. S. Atomic Energy Commission, in the Lawrence Radiation Laboratory.

BIBLIOGRAPHY

1. V. A. Borodin and Y. F. Dityakin, N.A.C.A. Tech. Memo. 1281 (1951). Translation from Priklodnaya Matematika I Mekhanika 13, No. 3,267 (1949).

2. J. L. Fick, H. E. Rea, and T. Vermeulen, Lawrence Radn. Lab. report UCRL-2545 (April 1954).

3. A. W. Hixson and A. H. Tenney, Trans. Am. Inst. Chem. Engrs. 31, 113 (1935).

4. F. Kneule, Chem. Ing. Tech. 28, 221 (1956).

5. G. E. Langlois, J. E. Gullberg, and T. Vermeulen, Rev. Sci. Instr. 25, 360 (1954).

6. S. A. Miller and C. A. Mann, Trans. Am. Inst. Chem. Engrs. 40, 709 (1944).

7. S. Nagata, I. Yamaguchi, and M. Harada, Chem. Eng. (Japan), 24, 742 (1960).

8. S. Nagata, T. Yokoyama, and H. Naka, Ibid. 17, 95, 98, 144 (1953).

9. Y. Oyama and K. Endoh, Ibid. 20, 666 (1956).

10. I. S. Pavlushenko, N. M. Kostin, and S. F. Matveev, Zhur. Priklad. Khim. 30, 1160 (1957).

11. I. S. Pavlushenko and A. V. Yanishevskii, Ibid. 31, 1348 (1958).

12. H. E. Rea, Jr. and T. Vermeulen, Lawrence Radn. Lab. report UCRL-2123 (April 1953).

13. J. H. Rushton, E. W. Costich, and H. S. Everett, Chem. Eng. Prog. 46, 395 (1950).

14. J. H. Vanderveen, Lawrence Radn. Lab. report UCRL-8733 (December 1960).

15. T. Vermeulen, G. M. Williams, and G. E. Langlois, Chem. Eng. Prog. 51, 85-F (1955).

16. J. Weisman and L. E. Efferding, A.I.Ch.E. Journal 6, 419 (1960).

17. L. H. Weiss, J. L. Fick, R. H. Houston, and T. Vermeulen, Lawrence Radn. Lab. report UCRL-9787 (September 1962).

18. T. N. Zwietering, Chem. Eng. Sci. 8, 244 (1958).

NOTATION

a = an exponent (Equations 4 and 6)

d_o = mean droplet diameter at impeller tip (Equation 7)

d_p = mean particle diameter of dispersed phase

G = agitator geometry group, dimensionless, LW/TH

g = acceleration of gravity

H = tank height

h = fractional tank height, dimensionless

h_B = fractional tank height of boundary between dispersible (but undispersed) phase and emulsion

L = impeller diameter

N = stirring speed, revolutions/ unit time

N_{Fr} = Froude Number, $N^2L\rho/g\Delta\rho(1 - \varphi)$

N_{Re} = Reynolds Number, $NL^2\rho/\mu_m$

N_{rel} = relative stirring speed (Figure 10)

N_{We} = Weber Number, $N^2L^3\rho/\sigma$

n = an exponent (Equation 6)

T = tank diameter

TMI = theoretical mixing index, $1/(1 + \kappa)$

V_j = local continuous-phase velocity

V_p = local dispersed-phase velocity, relative to continuous phase

W = impeller width

$\Delta\rho$ = density difference, $\rho_c - \rho_d$

κ = inhomogeneity parameter

μ_c = continuous-phase viscosity

μ_d = dispersed-phase viscosity

μ_m = mixture viscosity,

$$\frac{\mu_c}{(1 - \bar{\varphi})^{3/2}} \left[1 + \frac{\bar{\varphi}(\mu_d - \mu_c)}{\mu_d + \mu_c} \right]^{3/2}$$

ρ_c = continuous-phase density

ρ_d = dispersed-phase density

$\bar{\rho}$ = $\rho_c + \bar{\varphi}\,(\rho_d - \rho_c)$

σ = interfacial tension

φ_{max} = maximum volume-fraction of dispersed phase

φ_s = local volume-fraction of dispersed phase

$\bar{\varphi}$ = bulk-average volume-fraction of dispersed phase

Captions for Figures

Figure 1. Computed Dispersed-Phase Distributions (Exponential Model)

Figure 2. The Exponential Distribution Model (Theoretical)

Figure 3. Criterion for Kappa-Control of h_B

Figure 4. Computed Dispersed-Phase Distributions with Kappa-Control

Figure 5. Effect of κ and Dispersion-Controlled h_B upon φ_{max}, at Several Values of φ

Figure 6. Agitation Apparatus

Figure 7. Observed Dispersed-Phase Volume Fraction vs. Radial Position

Figure 8. Correlation for κ

Figure 9. Correlation for $h_B/\bar{\varphi}$

Figure 10. Relative Effect of Agitator Speed in the Two Types of h_B Control

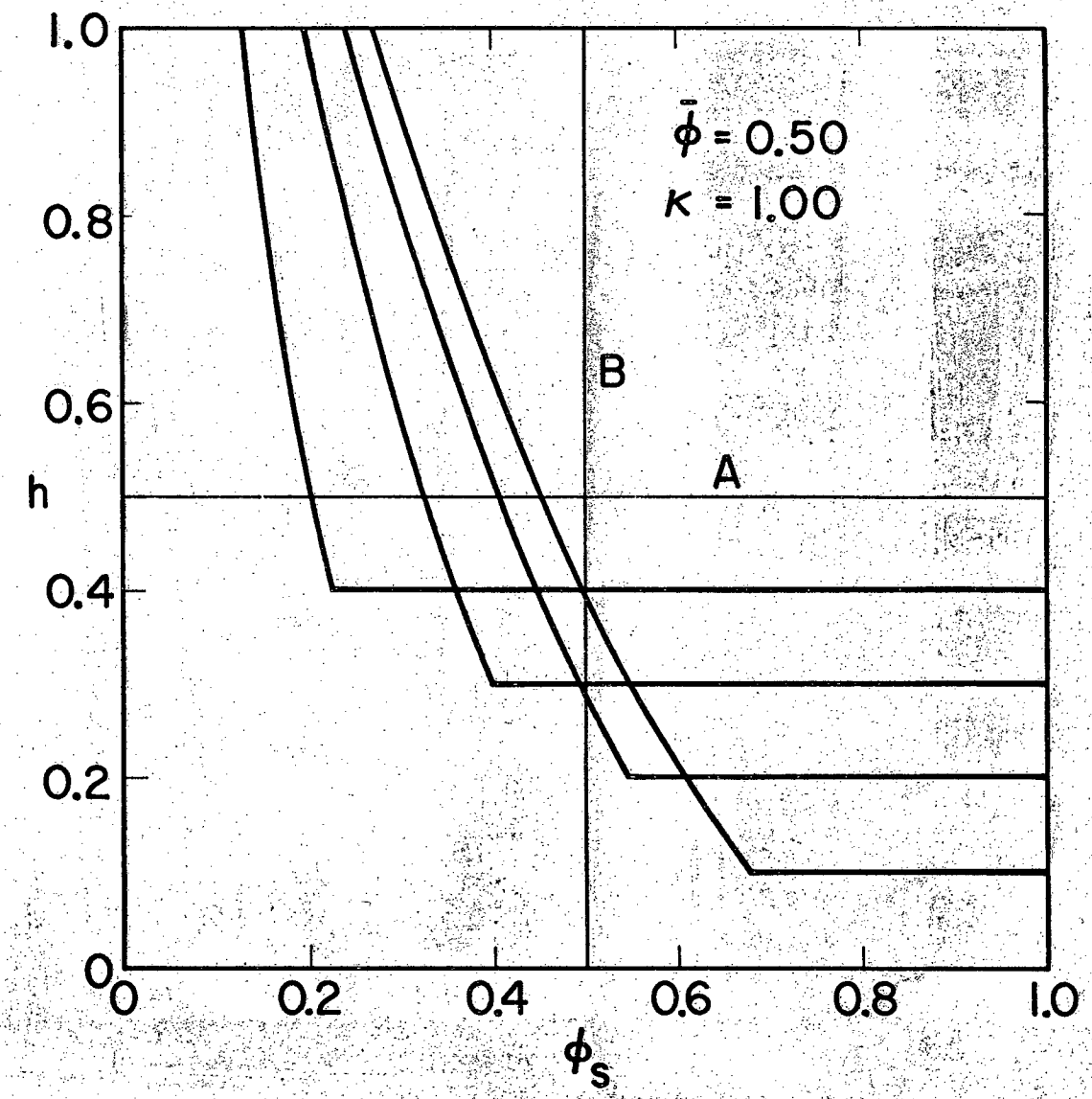

Figure 1. Computed Dispersed-Phase Distributions (Exponential Model)

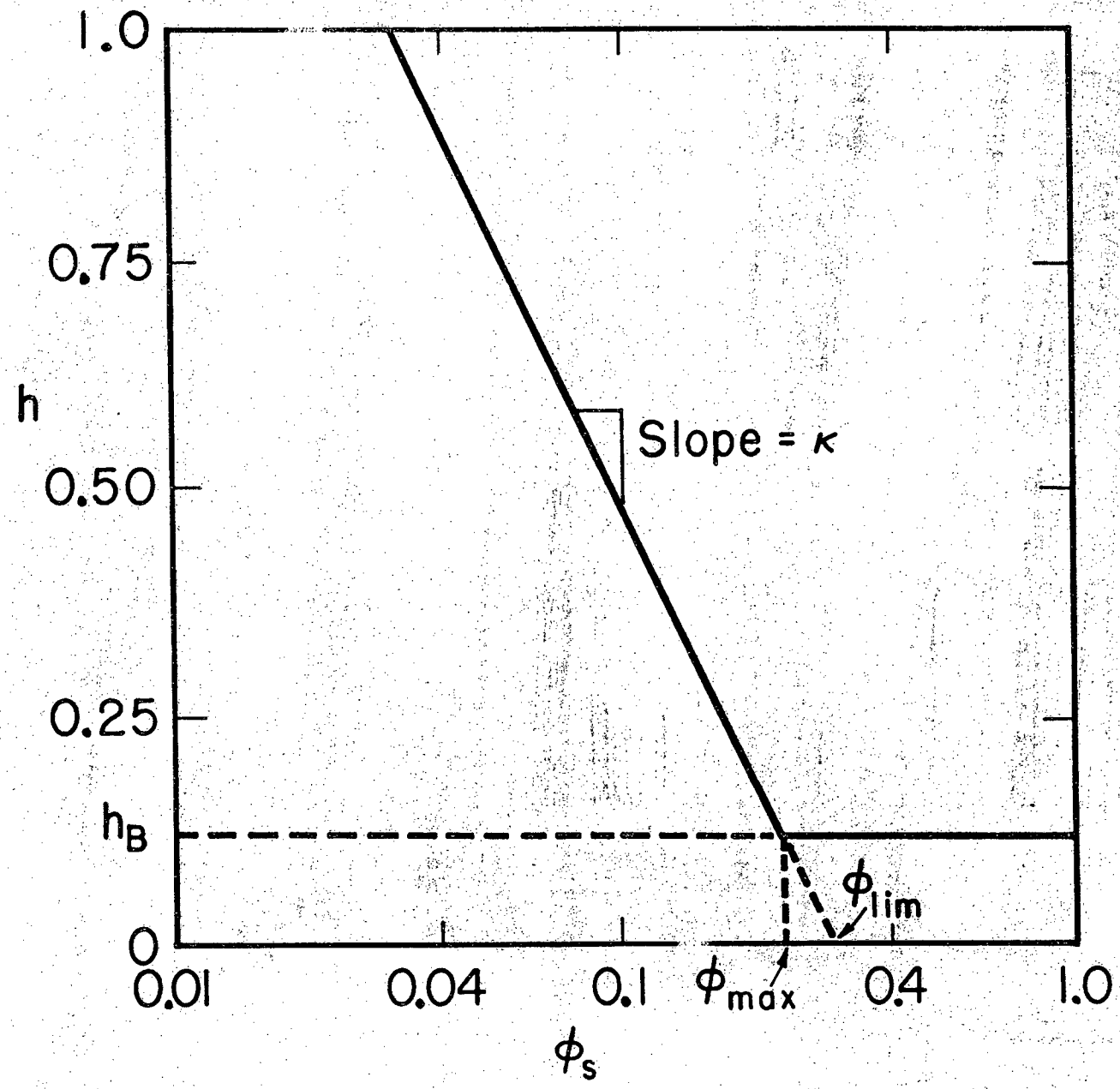

Figure 2. The Exponential Distribution Model (Theoretical)

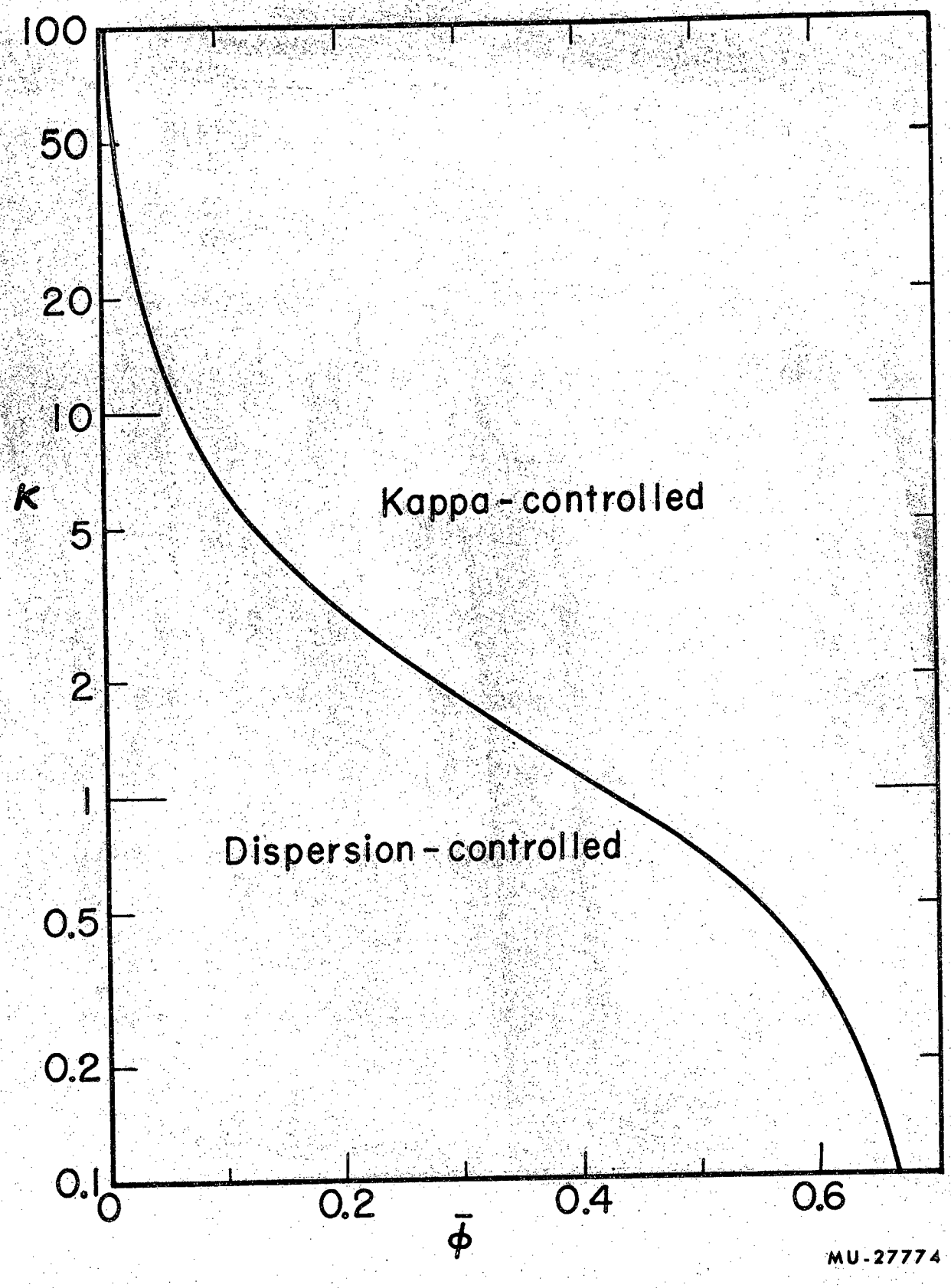

Figure 3. Criterion for Kappa-Control of h_B

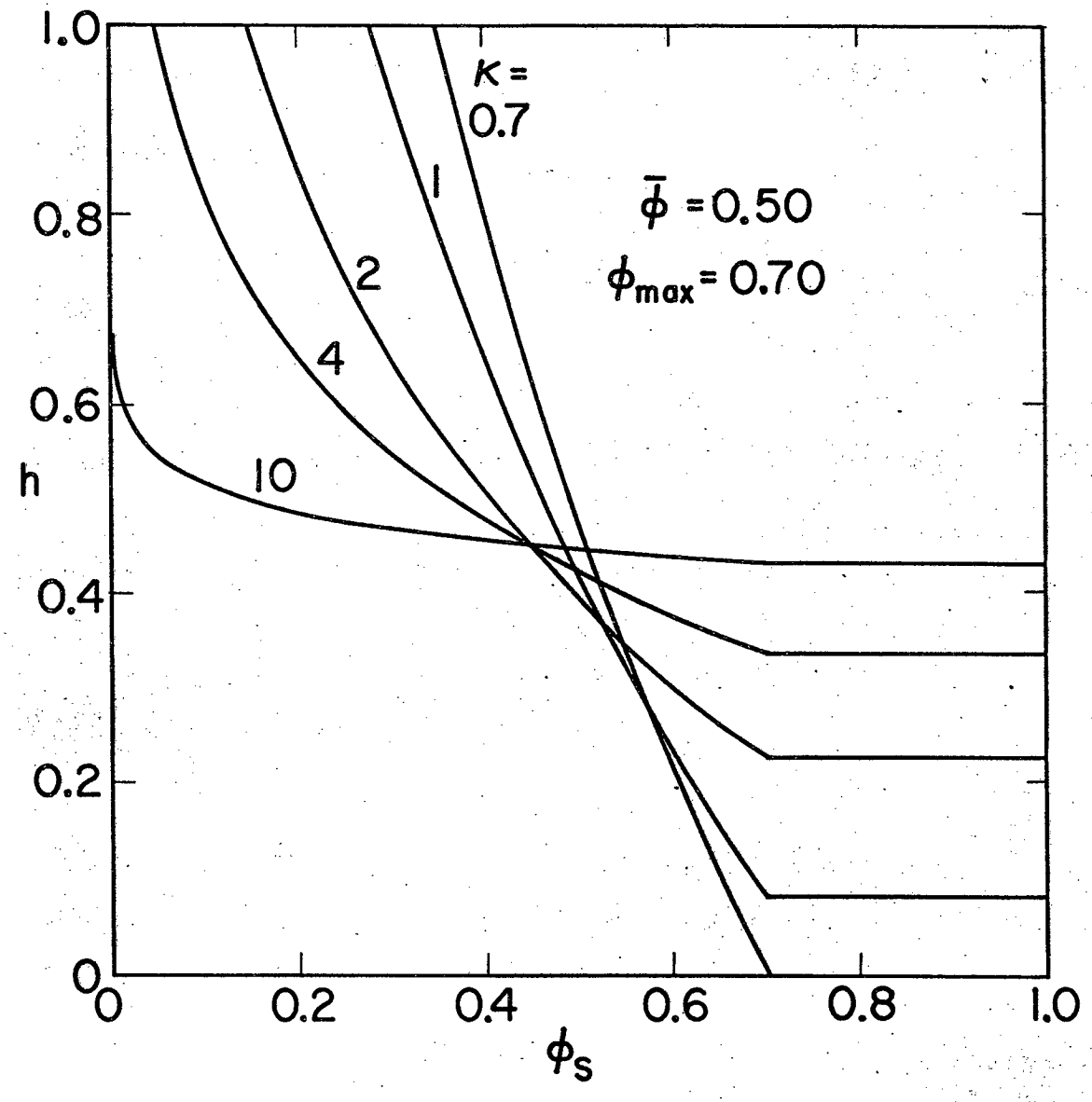

Figure 4. Computed Dispersed-Phase Distributions with Kappa-Control

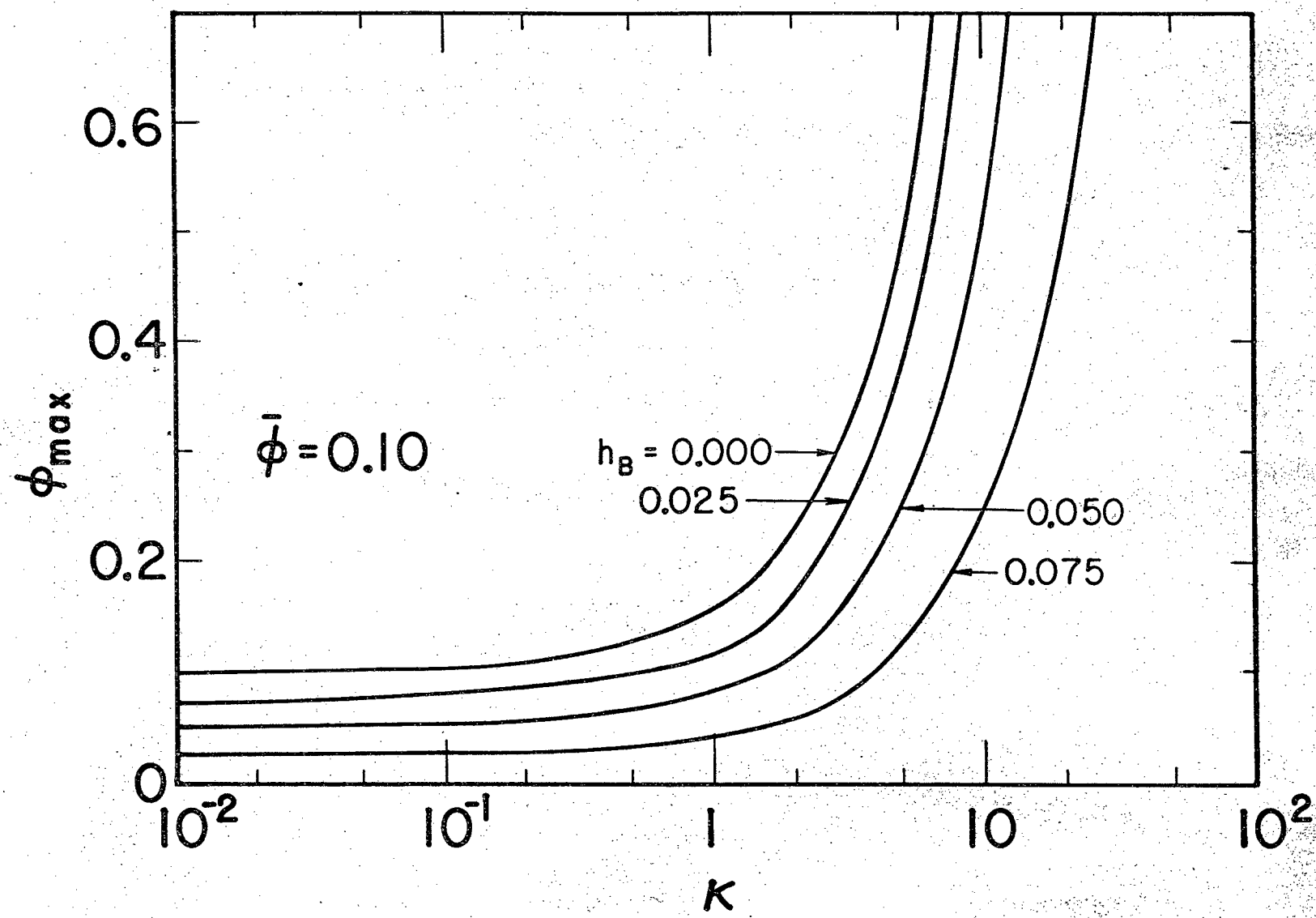

(a)

Figure 5. Effect of κ and Dispersion-Controlled h_B upon ϕ_{max}, at Several Values of $\bar{\phi}$

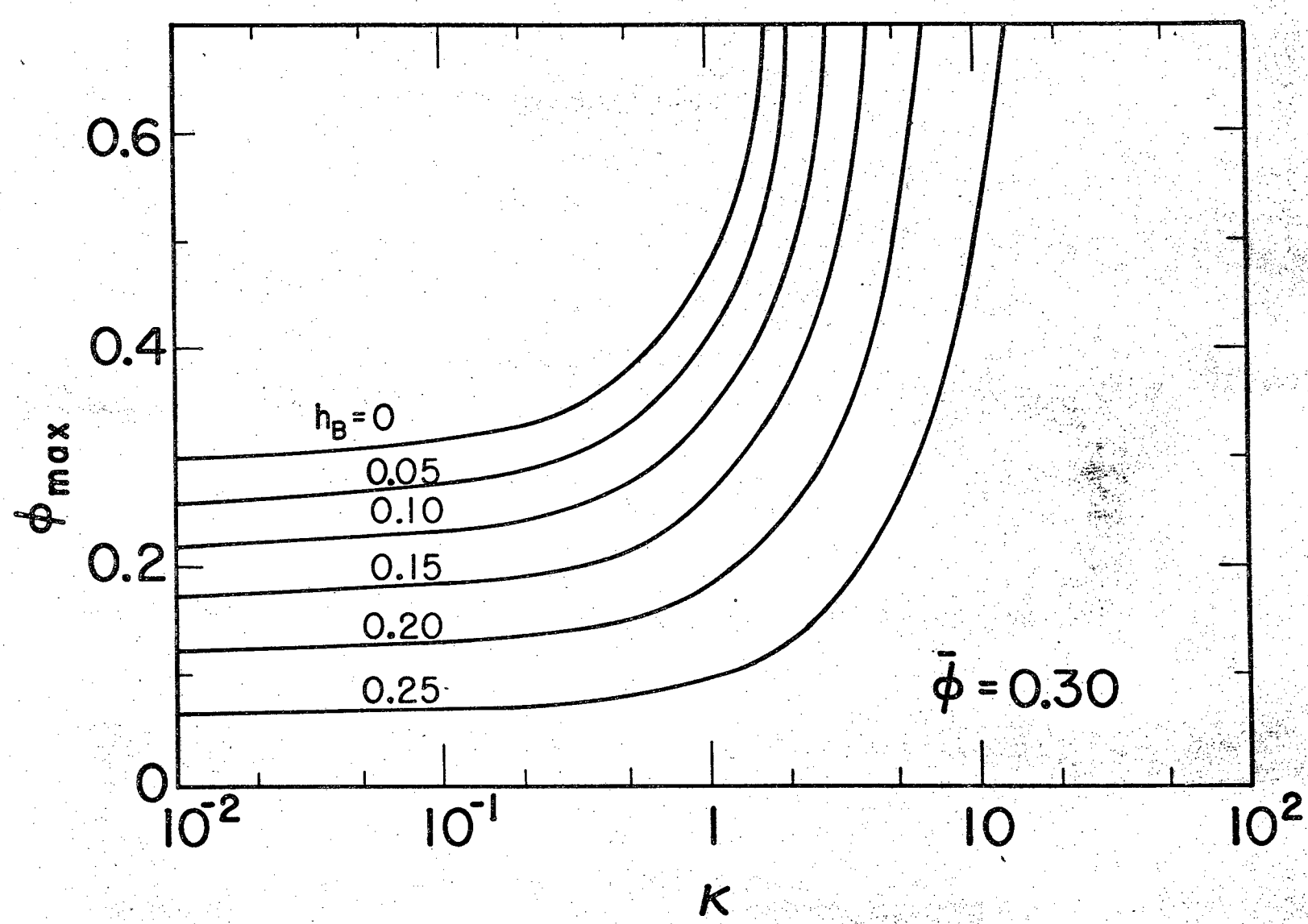

(b)

Figure 5. Effect of κ and Dispersion-Controlled h_B upon ϕ_{max}, at Several Values of $\bar{\phi}$

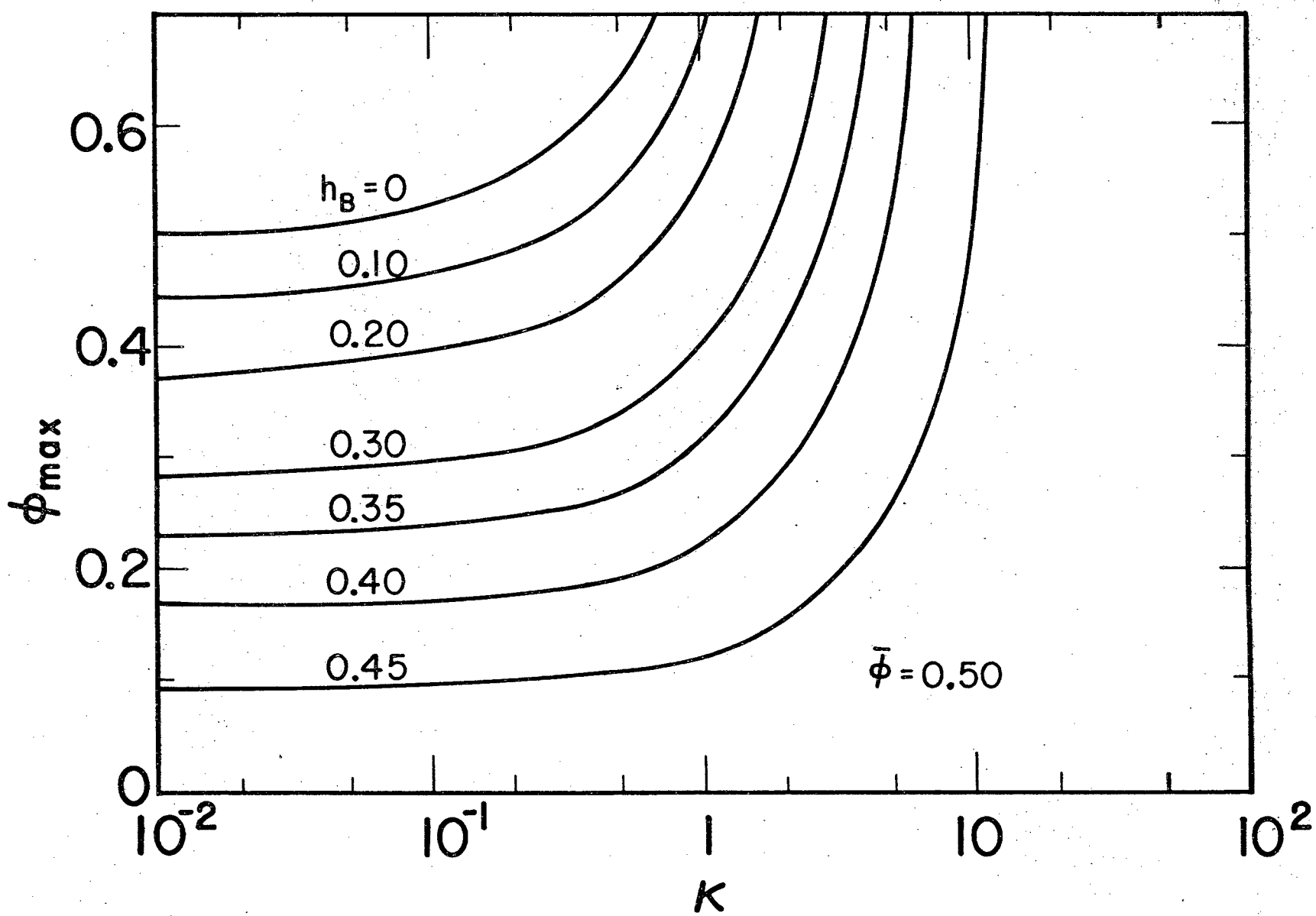

(c)

Figure 5. Effect of κ and Dispersion-Controlled h_B upon ϕ_{max}, at Several Values of $\bar{\phi}$

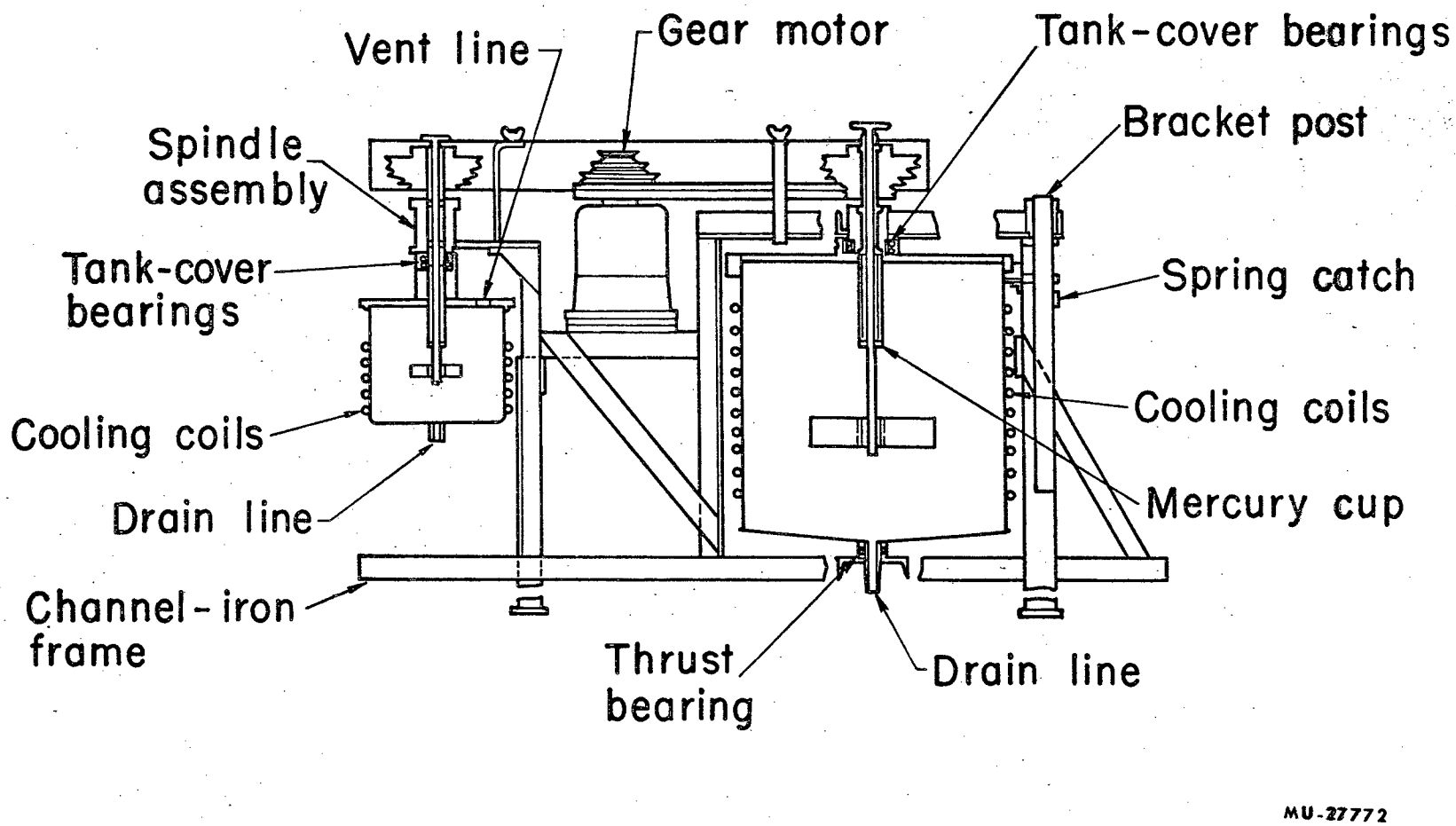

Figure 6. Agitation Apparatus

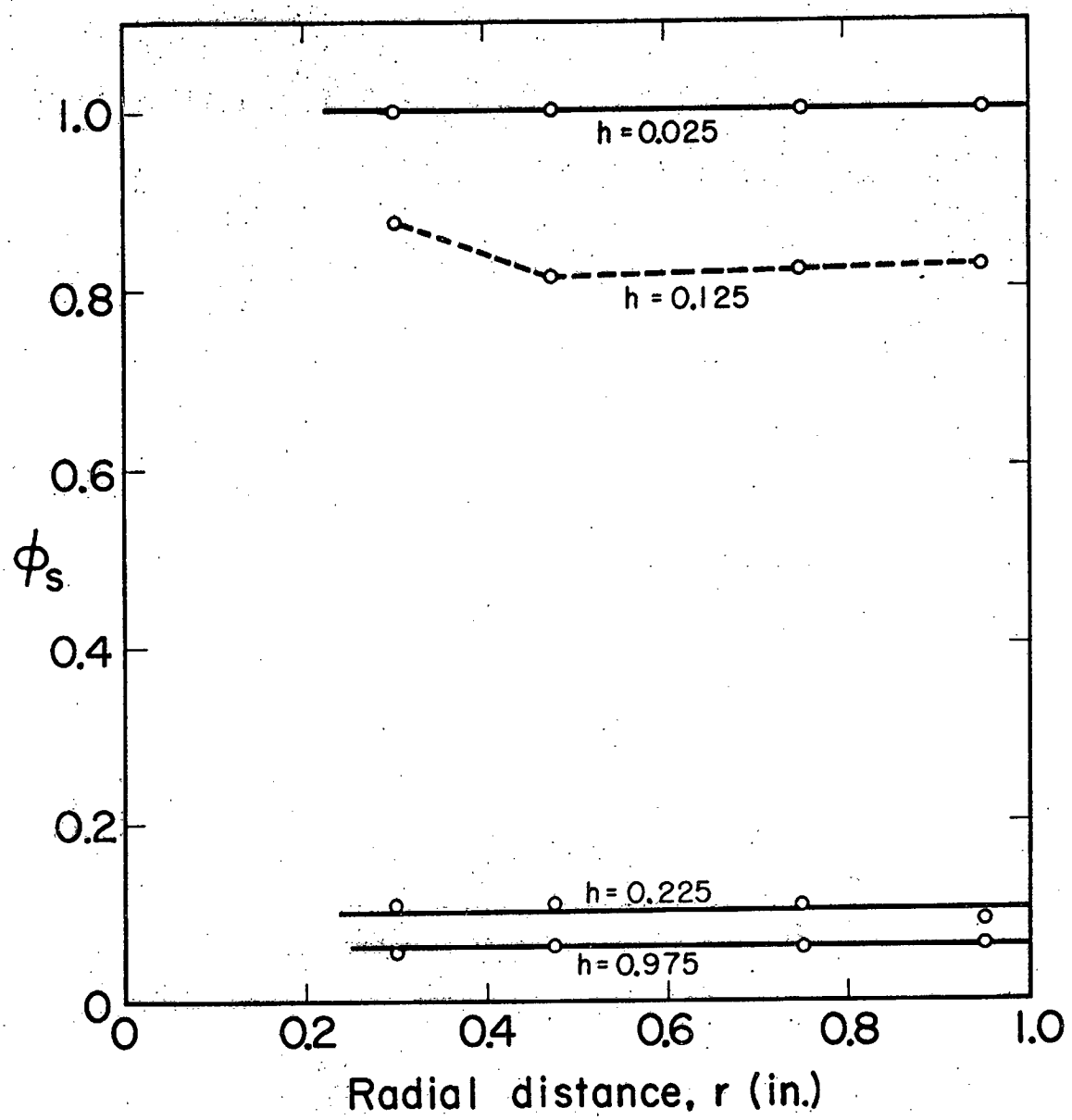

Figure 7. Observed Dispersed-Phase Volume Fraction vs. Radial Position

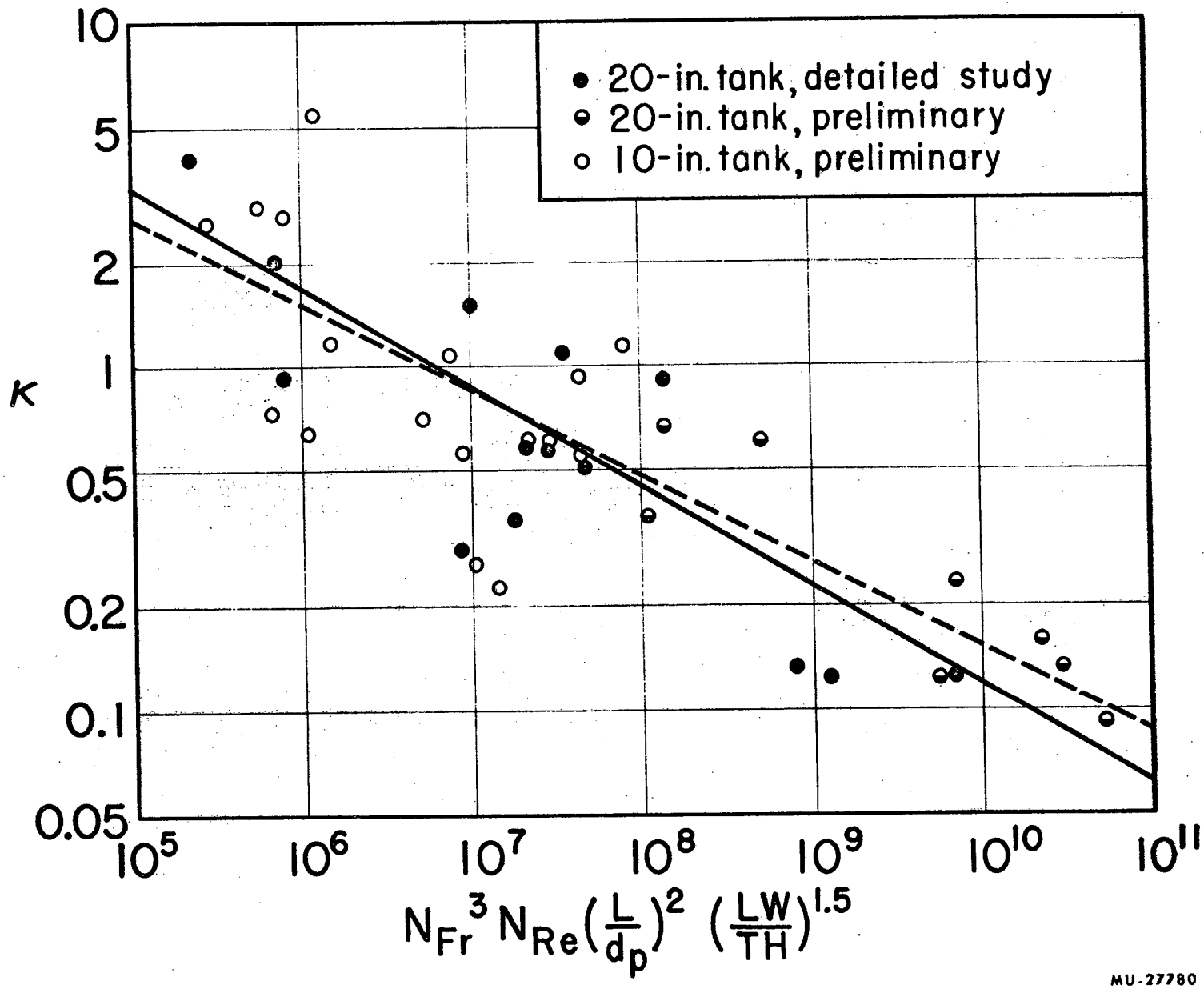

Figure 8. Correlation for κ

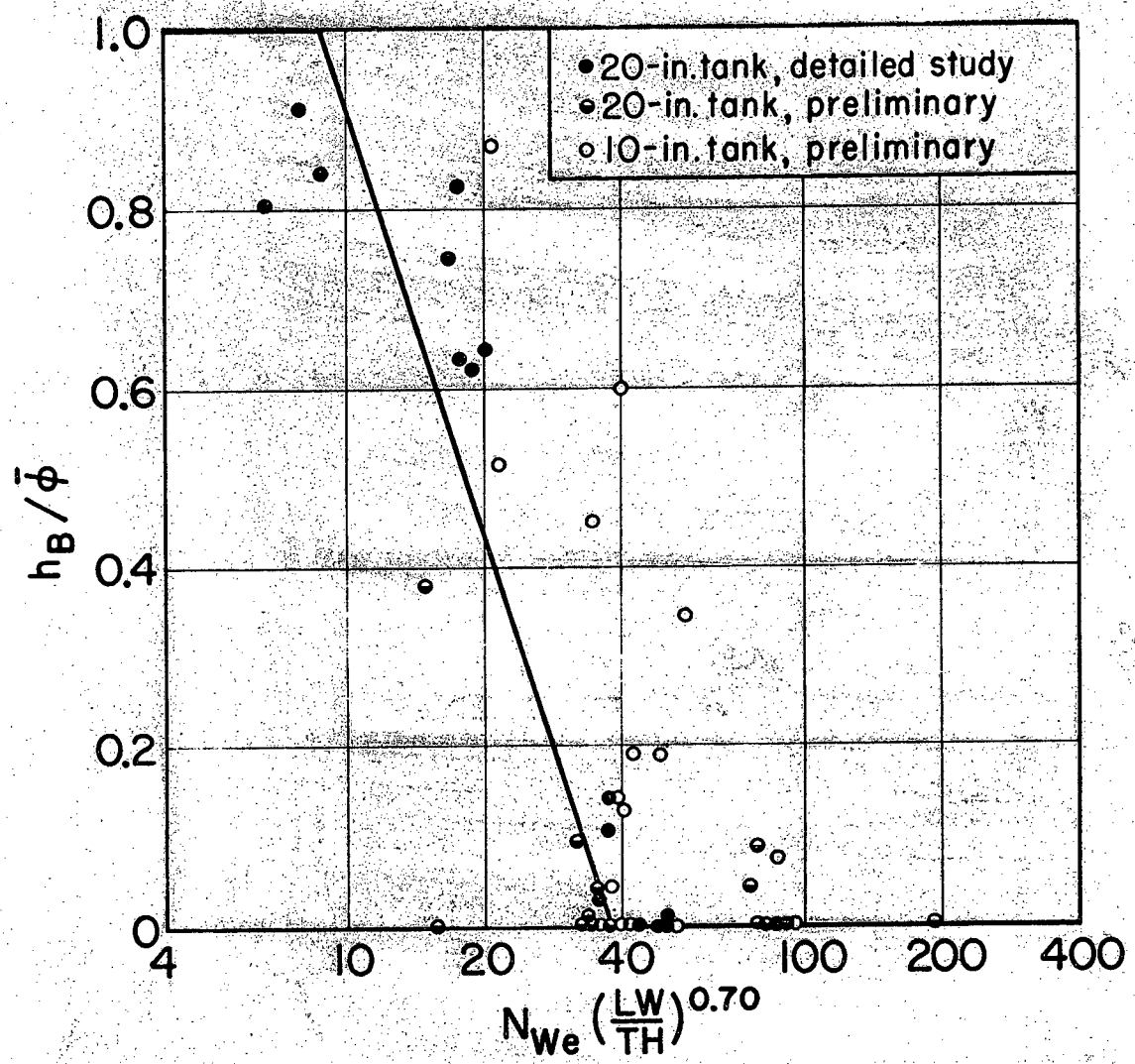

Figure 9. Correlation for $h_B/\bar{\varphi}$

MUB-1262

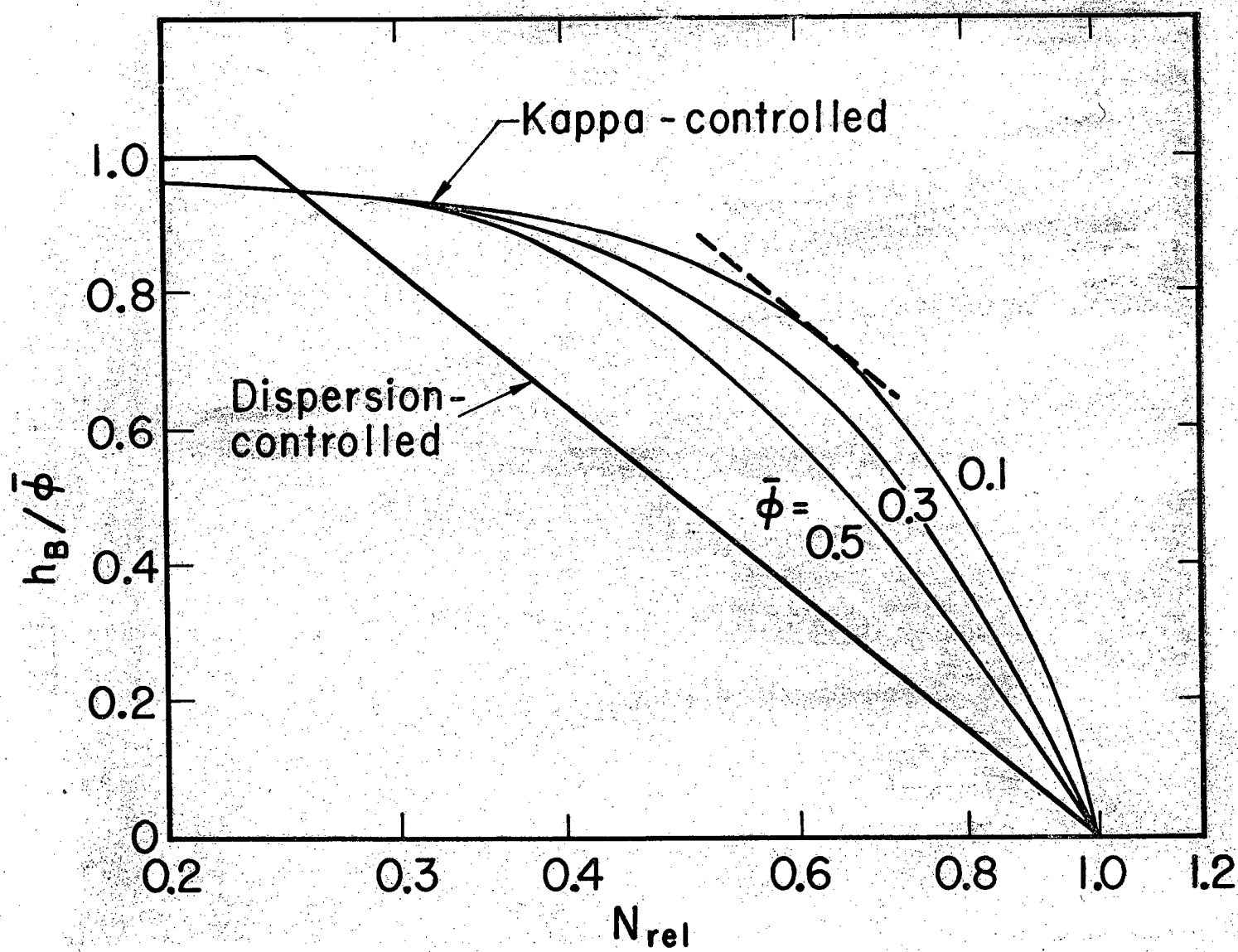

Figure 10. Relative Effect of Agitator Speed in the Two Types of h_B Control

This report was prepared as an account of Government sponsored work. Neither the United States, nor the Commission, nor any person acting on behalf of the Commission:

A. Makes any warranty or representation, expressed or implied, with respect to the accuracy, completeness, or usefulness of the information contained in this report, or that the use of any information, apparatus, method, or process disclosed in this report may not infringe privately owned rights; or

B. Assumes any liabilities with respect to the use of, or for damages resulting from the use of any information, apparatus, method, or process disclosed in this report.

As used in the above, "person acting on behalf of the Commission" includes any employee or contractor of the Commission, or employee of such contractor, to the extent that such employee or contractor of the Commission, or employee of such contractor prepares, disseminates, or provides access to, any information pursuant to his employment or contract with the Commission, or his employment with such contractor.